DEVELOPMENT OF A TEMPERATURE-DEPENDENT RADAR REFLECTIVITY TO SNOWRATE RELATIONSHIP FOR THE S-BAND

Jonathan P. Wolfe[1], Jefferson R. Snider[2] and Bart Geerts[2]
[1]National Weather Service, Portland, Oregon, USA
[2]*Department of Atmospheric Science, University of Wyoming, Laramie, Wyoming, USA*

ABSTRACT

Weather radar offers a practical way of estimating snowfall rate with high spatial and temporal resolution. Such remotely-sensed snowrates are useful for weather advisory and hydrometeorology. In either application a relationship between equivalent radar reflectivity (Z_e) and water equivalent snowrate (S) is needed. Furthermore, this relationship should be tuned to the location and cloud type of interest. The leading coefficient in the relationship $Z_e = \alpha \cdot S^{\beta}$ can be shown to vary with temperature-dependent properties of the snowflake size distribution. We describe measurements, and a statistical analysis, leading to a value for α which can be applied to wintertime upslope storms occurring in southeastern Wyoming, and report a positive correlation between α and surface temperature. This temperature-dependence is suggestive of a process which produces an inverse relationship between snowflake concentration and temperature, e.g., primary ice nucleation.

1. INTRODUCTION

In western North America snowfall accumulations are measured by a network of surface snowfall gages; including measurements made at weather service offices, snow telemetry pillow sites (SNOTEL), and by Community Collaborative Rain, Hail and Snow (CoCoRaHS) network. In spite of the large number of these precipitation monitoring sites, the network cannot resolve the spatial and temporal variability of precipitation. This challenge is vexing when quantifying either rainfall or snowfall, but in the case of snowfall there is the additional complication of measurement bias (Groisman and Legates, 1994).

Radar is an alternative to a denser network of precipitation gages. Measurements of snowfall rate (S) are derived with high spatial and temporal resolution via radar measurement of the equivalent reflectivity factor (Z_e) and a reflectivity-to-snowrate relationship (Rasmussen et al. 2002; Fujiyoshi et al. 1990; Boucher and Weiler 1985). A disadvantage of this approach, particularly in mountainous regions of the western US, is that terrain limits radar coverage (Pellarin et al. 2002). Because of these limitations a triad of measurement systems – radar, precipitation gages and SNOTEL – is envisioned as components of an improved snowrate and snow accumulation measurement effort (Wetzel et al. 2004).

Radar has been used to derive precipitation rate for over 60 years (Marshall et al., 1947), but variability in the relationship between radar reflectivity and precipitation rate has lead to deemphasis of radar remote sensing, particularly when examining snowfall. In the commonly used parameterization $Z_e = \alpha \cdot S^{\beta}$, where α and β are fitted values, α varies by an order of magnitude and β varies by +/- 15% (Rasmussen et al. 2003; Fujiyoshi et al. 1990). It was shown by Rasmussen et al. (2003) that the theoretical value of β is 1.7, however, the semi-empirical work of Sekhon and Shrivastava (1970) indicates β = 2.2. Here, we attempt to decrease the variability of the Z_e-S relationship by taking one of the fit coefficients to be a function of ambient temperature. Our study is guided by a simple

theory which predicts that β is a constant and that α varies positively with temperature.

2. MEASUREMENTS

2a. Measurement Site

Three measurement systems were used in this study. Their focus was a surface site located 25 km northwest of Cheyenne, Wyoming. The surface site is located on the eastern foothills of the Laramie Range at latitude 41° 15' 40" N and longitude 105° 03' 52" W at an elevation of 2092 m. Observations made at the surface site included snowrate, temperature and wind speed from the Hotplate precipitation sensor TPS-3100 (Rasmussen et al. 2002; Yankee Environmental Systems, Inc.) and temperature and wind speed from a Vaisala weather station WXT510 (Vaisala, Inc. 2005). Data from the surface-site sensors were recorded once per second. Four upslope snowstorms were studied during the winter of 2006 (March 8, March 12, March 19 and March 20).

2b. Hotplate Snowrate Sensor

The Hotplate consists of two vertically stacked 13 cm (diameter) circular plates mounted on a pedestal. The Hotplate control circuitry and the plate heating elements are designed to maintain the temperature of the plates at 90 ℃, adjusting for convective heat loss which removes heat from both plates, and for the heat demand of the top plate due to snowfall. The power difference between the two plates is used to compute the precipitation rate expressed as a one-minute and five-minute running average. If the value of the 5 minute running average exceeds 0.25 mm hr^{-1}, a provisional precipitation rate is output as a 1 minute running average; otherwise, the provisional precipitation rate is reported as 0 mm hr^{-1}. The provisional rate is divided by a windspeed-dependent catch efficiency and this corrected precipitation rate is output once per second (Rasmussen et al., 2005). Our Hotplate was purchased from Yankee Environmental Systems (Turner Falls, MA) in 2005 and utilized the firmware version 2.6.

We evaluated the accuracy of the Hotplate-derived precipitation rate, and the time-response of the Hotplate, by randomly distributing uniform-sized water drops (2 mm diameter) across the top plate surface. These laboratory-based studies reveal good agreement between our lab-based precipitation rate standard and the values reported by the Hotplate. On average, the absolute departure from the standard was 0.03 mm hr^{-1} for standard values between to 1 and 2.4 mm hr^{-1}. The lab tests also reveal that the Hotplate can respond to the onset of precipitation in 135 s (Wolfe 2007).

During daytime conditions the Hotplate-derived values of air temperature were positively biased by ~2 ℃ relative to the Vaisala WXT510; consequently, the Vaisala measurements of temperature were used in this analysis. The Vaisala and Hotplate wind speed measurements agreed, on average, within ±20%.

2c. Weather Surveillance Radar

Radar reflectivity measurements made over the surface site were acquired by the Cheyenne (Wyoming) Weather Surveillance Radar-1988 Doppler (Crum and Alberty 1993) hereafter referred to as the WSR. The WSR transmits and receives at a wavelength of 10 cm. The radar range gate, over the location of the surface site (azimuth angle = 299°, range=25 km), can be approximated as a nearly prostrate cylinder with length 1.0 km and diameter 0.40 km. Backscattered radiation detected by the radar is converted to an equivalent radar reflectivity factor, expressed in decibels, and is archived with azimuth angle, elevation angle, data and time. We utilized Level II WSR data obtained from the National Climatic Data Center. The radar scan strategy, which prescribes how the WSR probes the coverage volume, is selected by the radar operator. The two scan strategies used in this study are summarized in Table 1.

Table 1 - WSR scan strategies used in this study.

Volume Coverage Pattern Identifier	Time to complete a volume Scan, s	Elevation Angles, ^{o}
21	333	0.50, 1.45, 2.40, 3.35, 4.30, 6.00, 9.90, 14.60, 19.50
32	573	0.50, 1.50, 2.50, 3.50, 4.50

2d. Uncertainties

Here we discuss bias due to the possible misalignment of the Hotplate and WSR time series, plus bias due to our use of radar measurements made at the lowest WSR elevation angle (0.5 ^{o}). We synchronized the Hotplate and the surface site data acquisition system clocks to a reference at the beginning of the month of March 2006. Our comparison of these two clocks at the end of the month of March revealed that they had drifted by 300 s. Arbitrarily, the Hotplate clock was chosen for synchronizing the surface measurements (snowrate and temperature) to the Level II WSR data. In addition to the likely drift of the time reference at the surface site, the surface and radar data sets are misaligned because of the time it takes for snowflakes to fall from the elevation of the radar range gate to the surface. Figure 1 shows the cross section along the radial of the WSR that passes over the surface site with the 0.5° and 1.5° beam centers and the 0.5° half power beam width overlaid. It demonstrates that the snowflake fall distances range between 50 and 500 m for these two lowest elevation angles. Assuming a representative snowflake fall speed (1 m/s, Locatelli and Hobbs (1974)), the time mismatch could be as large as 500 s. When we did account for this time mismatch we found no evidence for an improvement in the correlation between the surface and WSR measurements. Hence, for this analysis we did not shift the two time series.

It is evident from Figure 1 that 50% of the 0.5° transmission is blocked by terrain. In contrast, the 1.5° transmission is not affected. This suggests that reflectivities from the 0.5° elevation angle could be negatively biased. This issue is discussed further in Section 4a.

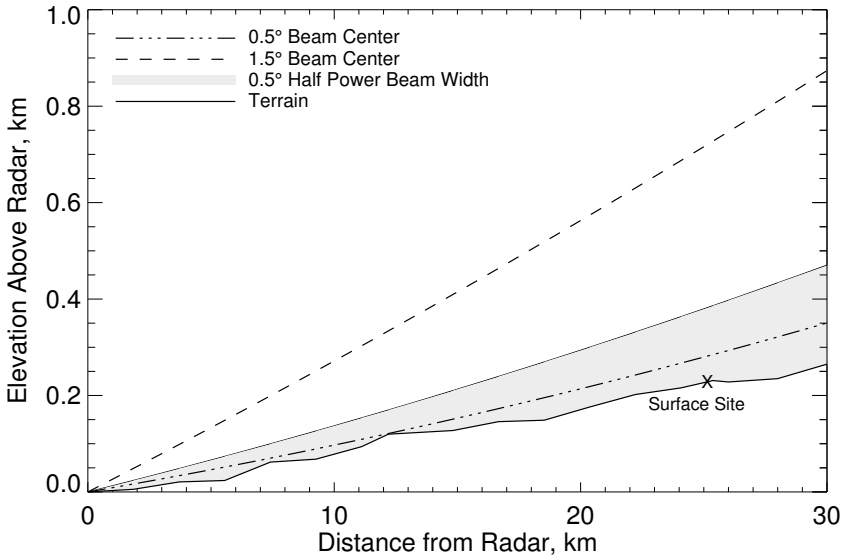

Figure 1 - Cross section of the terrain along the radial of the WSR that passes over the surface site assuming a standard profile of temperature, pressure and humidity.

3. THEORETICAL MOTIVATION

This work correlates measurements of surface snowrate (S), expressed as a water equivalent depth per unit time, with radar-derived values of the equivalent radar reflectivity factor (Z_e). The equation commonly used to describe this correlation is a power law of the form:

$$Z_e = \alpha \cdot S^{\beta} \qquad (\text{mm}^6\ \text{m}^{-3}) \qquad (1)$$

The coefficients α and β are often derived by regressing concurrent measurements of Z_e and S. Prior investigators have employed a variety of averaging techniques aimed at of minimizing statistical error due to atmospheric variability and instrument sensitivity issues (Super and Holroyd, 1998; Fujiyoshi et al. 1990; Rasmussen et al. 2003).

Rasmussen et al. (2003) describe how α and β vary with local conditions within the atmospheric volume that is probed by a WSR. For their theoretical analysis they assume that the snowflake size distribution function can be described by the exponential form proposed by Marshall and Palmer (1948) for rain. The function has the form $N(D) = N_o \cdot \exp(-\Lambda D)$, where N_o is the y-intercept of the function, Λ is the slope of the function and D represents the unmelted snowflake diameter. Following Rasmussen et al., we parameterize the snowflake density (ρ_S) in terms of a parameter (Ω) and the unmelted snowflake diameter ($\rho_S = \Omega / D$). In this parameterization ρ_S is the ratio of snowflake mass to its inscribed volume. Both Ω and ρ_S vary with environmental conditions, with the simplest three categorizations being 1) snowflakes with a temperature of 0 °C (wet snow), 2) snowflakes grown by the accretion of supercooled cloud droplets (rimed snow), and 3) snowflakes grown by either vapor diffusion or aggregation in an environment colder than 0 °C (dry snow). For the latter conditions, a representative value of Ω is 0.2 kg m/m^3 (Rasmussen et al., 2003; Liu and Illingworth, 2000). These two relationships (Marshall-Palmer and size-density) allowed Rasmussen et al. to derive a theoretical Z_e-S relationship. Here we restate their result for dry snow conditions

$$Z_e = 2.22 \cdot 10^{19} \cdot \frac{|K_i|^2}{|K_w|^2} \cdot \frac{\rho_w^{5/3}}{\rho_i^2} \frac{\Omega^{1/3}}{V_t^{5/3} \cdot N_o^{2/3}} \cdot S^{5/3}$$

$$(\text{mm}^6\ \text{m}^{-3}) \qquad (2)$$

In Equation (2), $|K_i|^2$ and $|K_w|^2$ are the moduli of the complex dielectric factors for ice and water, ρ_i and ρ_w are the corresponding bulk densities, and V_t is the snowflake terminal velocity. Moreover, all symbols on the right-side of the Equation 2 are expressed in terms of their meter-kilogram-second equivalent.

We extend Equation 2 by first noting that its derivation starts with separate developments for Z_e and S, leading to relationships which have S proportional to the second moment and Z_e proportional to the sixth moment of the of the Marshall-Palmer size distribution function. Furthermore, we note that these proportionalities require the assumptions that terminal velocity is a constant and that the scattering is described by Rayleigh theory. Finally, we note that the snowflake concentration is the zeroth moment of the Marshall-Palmer function. Using the same assumptions as are implicit in Equation 2 (Rayleigh scattering, Marshall-Palmer size distribution function and size-independent terminal velocity and size independent Ω), we derive an alternate form for the Z_e-S relationship

$$Z_e = 2.19 \cdot 10^{19} \cdot \frac{|K_i|^2}{|K_w|^2} \cdot \frac{\rho_w^2}{\rho_i^2} \cdot \frac{1}{V_t^2 \cdot N} \cdot S^2$$

$$(\text{mm}^6\ \text{m}^{-3}) \qquad (3)$$

Here N is the zeroth moment of the size distribution, i.e., the size-integrated concentration of snowflakes. Equation 3 demonstrates that Ω cancels out of the theoretical Z_e-S relationship, that β is a constant, and that α (the group of parameters multiplying S^2 in Equation 3) is a function of the cloud microphysical properties N and V_t. It also shows that α will be larger in cloud volumes containing lower concentrations of snowflakes. In addition, if snowflake concentrations vary inversely with temperature, as is observed in clouds containing ice generated by heterogeneous nucleation (primary ice generation; see, for example, Cooper (1986)) then it follows that α will be larger in cloud volumes observed at warmer temperatures.

The proceeding theoretical analysis of the power-law relationship between radar reflectivity and snowrate leads us to hypothesize that α is temperature dependent. We test that hypothesis.

4. RESULTS

4a. Beam Blockage

Bech et al. (2003) considered situations like that illustrated in Figure 1 and analyzed the effect of the beam blockage on the backscattered signal. We addressed this issue two ways. First, we analyzed the WSR radial velocity data, acquired as the lowest radar tilt angle (0.5°) and found no evidence for beam blockage along the radial between the WSR and the surface site. Second, we regressed the radar reflectivities acquired at the elevation angles 0.5° and 1.5° (over the surface site) and found no evidence for a shift between these when the WSR was operated in scan mode #32 (Table 1). A shift was detected when the WSR was operated in scan mode #31 but interpretation of this shift as beam blockage is complicated by the very weak correlation between the 0.5° and 1.5° reflectivities when operating in this scan mode. These analyses indicated that beam blockage did not significantly bias the reflectivity measurements acquired at 0.5°, at least when the WSR was operated in scan mode #32. In spite of this we remain suspicions about beam blockage at the lowest WSR elevation angle, even though a majority of the WSR measurements were acquired in the #32 scan mode. For this reason we fit the Z_e-S relationship using data collected at elevation angle 0.5°, at elevation angle 1.5°, and by combining data acquired at both elevation angles.

4b. Fitting

Three statistical methods were used to calculate α and each is described in the Appendix. The first minimizes the departure of Z_e from the line $Z_e = \alpha_1 \cdot S^2$, the second minimizes the departure of S^2 from the line $Z_e = \alpha_2 \cdot S^2$, and the third minimizes the departure of $\ln Z_e$ from a line of the form $\ln Z_e = \ln \alpha_3 + \ln S^2$. Also explained in the Appendix is the calculation of the standard errors: $\sigma_{\alpha 1}$, $\sigma_{\alpha 2}$ and $\sigma_{\alpha 3}$.

Figure 2 shows a plot of the Z_e-S pairs binned into three 4 °C temperature intervals starting at -12 °C and ending at 0 °C; colors represent the Coordinated Universal Time (UTC) date of the measurements. Data acquired at both WSR elevation angles (0.5° and 1.5°) is represented here. The figure shows that each temperature interval contains Z_e-S pairs from at least two of the four study days and that a majority of the data was acquired at temperatures warmer than -8 °C. Furthermore, a clear increase in α_3 with increasing temperature is evident. We focus on this particular value of α because the departure of the measured snowrates from the line $Z_e = \alpha_3 \cdot S^2$ is smaller than that for the two other fitting functions. Values of the departure, expressed as a average absolute snowrate error, are equal to 0.2, 0.6 and 0.5 mm/hr for the temperature bins -12/-8, -8/-4 and -4/0, respectively. These departures are noticeably smaller than those obtained for

the $Z_e = \alpha_1 \cdot S^2$ parameterization, and insignificantly smaller to that for the $Z_e = \alpha_2 \cdot S^2$ parameterization.

4c. Temperature-dependence of α

Figure 3 presents values for α_1, α_2, and α_3 as a function of temperature for the 0.5° and 1.5° elevation angles (left and middle panel) and for both angles (right panel). Values for α_3 are connected to illustrate the monotonic nature of its increase with temperature. The error bars extend from α minus one standard error to α plus one standard error.

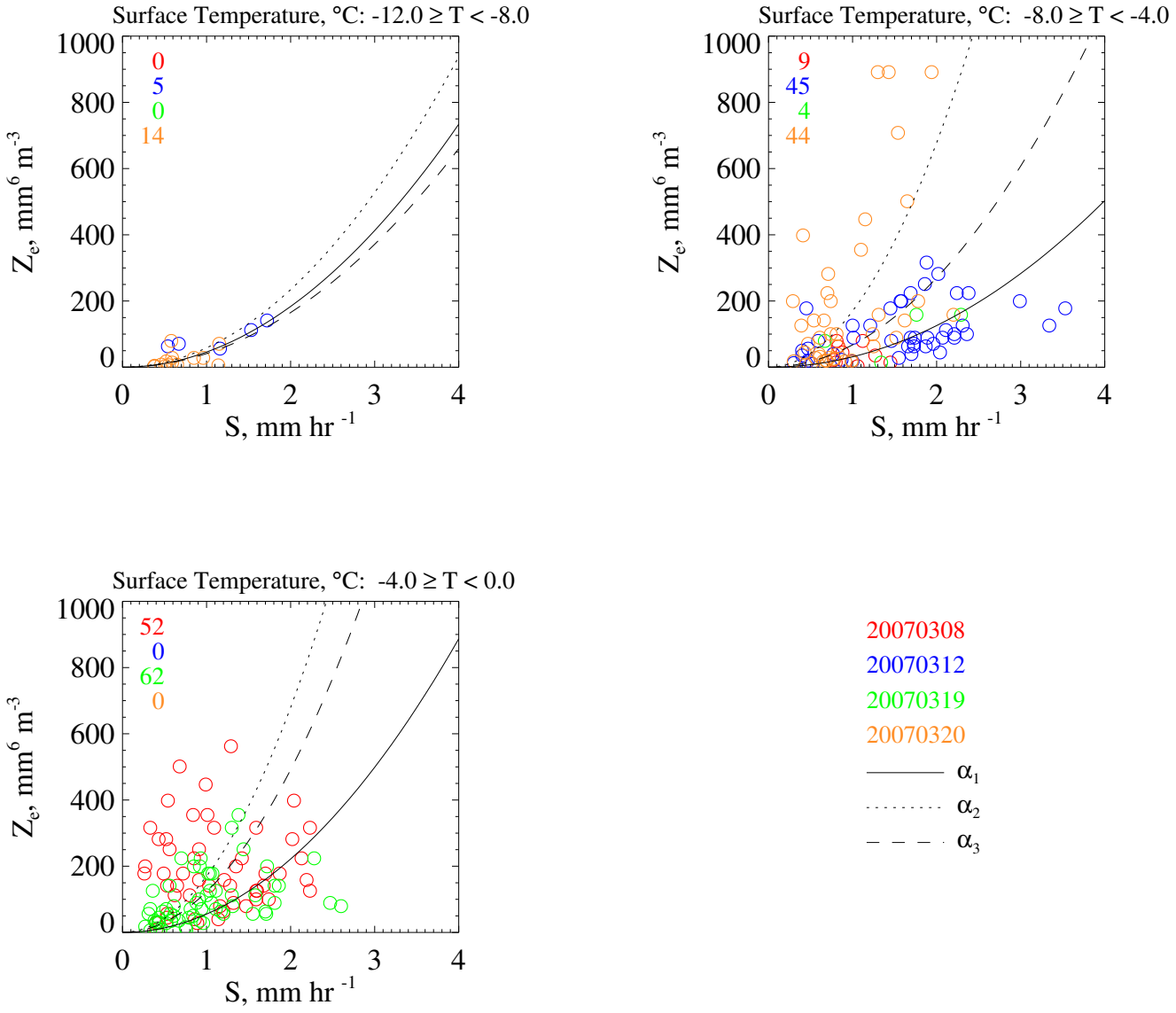

Figure 2 - Plots of Z_e-S pairs for three 4 °C temperature intervals beginning at -12 °C and ending with 0 °C. Data from both radar elevation angles (0.5° and 1.5°) is displayed. Also shown are the best-fit lines corresponding to α_1, α_2 and α_3. The number of data points from each day is shown in the upper-left corner of the panels.

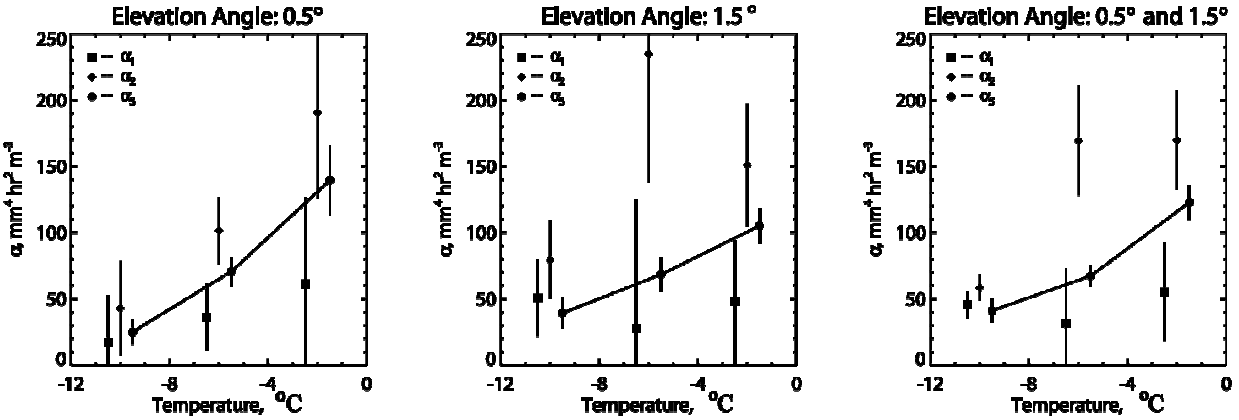

Figure 3 - Values for α_1, α_2, and α_3 versus temperature for the WSR elevation angles 0.5° (left panel) and 1.5° (middle panel). The right panel shows the result obtained by combining data from both elevation angles. Error bars extend from the fitted value minus the standard error to the fitted value plus the standard error. A line connects the temperature-dependent values of α_3.

4d. Validation

Table 2 shows the comparison of radar-derived snowfall accumulation (based on our temperature-dependent α_3 and radar data acquired at 0.5°) versus accumulations from the Community Collaborative Rain, Hail and Snow (CoCoRaHS) network. The CoCoRaHS measurements are reported every 24 hours and correspond to samples accumulated between from 7 am LST (day 1) and 7 am LST (day 2). Results shown in Table 2 are from the four closest CoCoRaHS sites and these are labeled by the distance (km), and by the direction (either to the south or east), from our surface site to the CoCoRaHS. Also compared are accumulations from the Hotplate and a radar-derived accumulation based on the values of α and β recommended by Super and Holroyd (1998) for snow in Denver, Colorado.

Table 2 shows that the best correspondence is between the Hotplate and the radar-derived accumulation based on the α_3 parameterization. This comparison tests our fitting procedure and highlights the point made is Section 4b where we show that α_3 is preferred over either α_2, or α_1, for estimating snowrate from reflectivity (i.e., the mean absolute snowrate departure is smallest for α_3). Also evident from Table 2 is the good agreement between our radar-derived accumulations and those based on Super and Holroyd (1998). There is an important difference between our data set and the data set analyzed by Super and Holroyd. We base our fitting on 235 sample pairs (Figure 2); neither Z_e or S is averaged. In contrast, Super and Holroyd used 458 hourly-averaged snowrate values, acquired over two winter seasons, to build their Z_e- S parameterization for Denver, CO. Our work indicates that parameterizations can be constructed with snowrate measurements from the Hotplate and suggests that improvements may result because of the faster response characteristic of the Hotplate compared to that of conventional snowrate gauges.

The comparison to the CoCoRaHS network shows reasonable agreement on March 8, in particular for the comparison to the 13-E-b site, and on March 19 in the comparison to the 6-S site. On March 12 all of the CoCoRaHS reported substantially larger snorates.

Table 2 - Comparison of 24 hr accumulations expressed in millimeter of water equivalent precipitation

Accumulation Method	7 am (LST) to 7 am (LST)			
	March 8	March 12	March 19	March 20
CoCoRaHS 6-S	NA	6.6	5.6	NA
CoCoRaHS 8-E	2.3	6.9	10.2	0.5
CoCoRaHS 13-E-a	2.8	6.4	6.9	0.5
CoCoRaHS 13-E-b	4.8	7.6	7.4	NA
Hotplate	5.4	4.2	3.2	0.0
Radar-estimated using $Z_e = \alpha_3 \cdot S^2$ (this work)	5.1	3.6	5.0	0.0
Radar-estimated using $Z_e = 130 \cdot S^2$ (Super and Holroyd, 1998)	4.5	3.3	3.6	0.0

NA – not available
LST – local standard time

6. SUMMARY

This study examined the role of temperature in the relationship between snowrate (S) and radar reflectivity (Z_e). In our examination of this temperature-dependence we prescribed the value of the exponent in the fitting equation (Equation 1). It is shown, both theoretically and empirically, that the leading term in the fitting equation (α) increases with temperature. We also show that the radar-derived accumulations agree with the Hotplate accumulations, and that the former agree with subset of the CoCoRaHS measurements made in the vicinity of our surface site. The snowrates reported in this study are relatively small (<4 mm/hr) and are subject to error in both the Hotplate and in the WSR measurements. Both errors are discussed and a formulism is established for estimating the best-fit coefficient and its standard error.

The assertion that α is solely dependent on snowflake number concentration (Equation 3), and that this dependency drives the temperature dependence we report, can be criticized on several fronts. In particular, criticism can be leveled against the assumptions that snowflake terminal velocity is a constant that the vigor of ice nuclei activation is insensitive to either aerosol background or cloud depth (i.e., cloud top temperature). Since the latter of these should vary with cloud top height, something which can be diagnosed using height-resolved WSR measurements, there is some potential for refinement. In this way the technique we propose – using fast response snowrate measurements in combination with the WSR – may help to improve region-wide updates of snowfall.

7. APPENDIX

Described here are the statistical tools we used to derive three estimates of the coefficient in Equation 1. Each approach starts with the paired sets Z_e and S^2. The first takes Z_e to be the dependent variable and employs a least squares procedure called "curvefit" (Integrated Data Language, RSI Inc.) which iteratively minimizes the sum of the square of the departure of the data points from the best-fit line. The calculation proceeds via three steps: 1) A provisional value of α_1 is produced when "curvefit" is initialized with equal weighting applied to all data points, and the resulting α_1 is used to evaluate weights as the either the reciprocal of the actual departure or 0.01 m^3/mm^6. The larger of the two values is chosen as the

weight. 2) Curvefit is applied again, with weights set equal to the value chosen in step #1, and the new estimate of α_1 is used to update the weights as in the #1 step. 3) Step #2 is repeated until the absolute relative change of α_1 is less than 0.01. It can be shown that these steps converge to a solution which minimizes the sum of the absolute value of the departures, as opposed to the least squares approach of minimizing the sum of the square of the departures, and is thus preferred in a situation such as this where there are outlier data values (Aster et al., 2005).

The value of α_2 is derived as described for α_1, however S^2 is taken to be the dependent variable and the resulting fit coefficient (γ_2) is converted to an "alpha" (i.e., $\alpha_2 = 1/\gamma_2$). The lower-limit for the weight (steps #1 and #2) is taken to be 1 hr mm^{-1}.

The values of α_1 and γ_2 are used to derive the standard errors as

$$\sigma_{\alpha 1} = \sqrt{\frac{\sum (Z_e - \alpha_1 \cdot S^2)^2}{N \cdot \left(\sum S^4 - \frac{1}{N} \cdot (\sum S^2)^2 \right)}} \qquad \text{(A1)}$$

$$\sigma_{\gamma 2} = \sqrt{\frac{\sum (S^2 - \gamma_2 \cdot Z_e)^2}{N \cdot \left(\sum Z_e^2 - \frac{1}{N} \cdot (\sum Z_e)^2 \right)}} \qquad \text{(A2)}$$

$$\sigma_{\alpha 2} = \frac{1}{\gamma_2^2} \cdot \sigma_{\gamma 2} \qquad \text{(A3)}$$

Here N is the total number of data points and Equation A3 employs propagation of error (Young, 1962) to derive the α_2 standard error from the values of γ_2 and $\sigma_{\gamma 2}$.

The third approach is based on the principle of maximum likelihood applied to logarithmically transformed sets of Z_e and S^2. From consideration of the principle of maximum likelihood (Young, 1962) it can be shown that the fit coefficient is

$$\alpha_3 = \exp\left(\left\langle \ln Z_e \right\rangle - \left\langle S^2 \right\rangle \right) \qquad \text{(A4)}$$

Here $\left\langle \ln Z_e \right\rangle$ and $\left\langle \ln S^2 \right\rangle$ are averages of the log-transformed sets of Z_e and S^2 and the standard error is

$$\sigma_{\alpha 3} = \sqrt{\alpha_3^2 \cdot \frac{\sum (\ln Z_e - \ln \alpha_3 - \ln S^2)^2}{N^2}} \qquad \text{(A5)}$$

6. REFERENCES

Aster, R., B. Borchers, and C. Thurber, 2004: *Parameter Estimation and Inverse Problems*, Academic Press.

Bech, J., B. Codina, J. Lorente, and D. Bebbington, 2003: The Sensitivity of Single

Polarization Weather Radar Beam Blockage Correction to Variability in the Vertical Refractivity Gradient, *J. Atmos. Oceanic Technol.*, **20**, 845–855.

Cooper, W. A., 1986: Ice initiation in natural clouds. *Precipitation Enhancement—A Scientific Challenge, Meteor. Monogr.,* No. 21, Amer. Meteor. Soc., 29–32.

Crum, T., and R. Alberty, 1993: The WSR-88D and the WSR-88D operational support facility. *Bull. Amer. Meteor. Soc.*, **74**, 1669-1687.

Fujiyoshi, Y., T. Endoh, T. Yamada, K. Tsuboki, Y. Tachibana and G. Wakahama, 1990: Determination of a *Z-R* relationship for snowfall using a radar and high sensitivity snow gauges. *J. Appl. Meteor.*, **29**, 147–152.

Joss J., and A. Waldvogel, 1990: Precipitation measurement and hydrology. Radar in Meteorology: Battan Memorial and 40th Anniversary Radar Meteorology Conference, D. Atlas, Ed., Amer. Meteor. Soc., 577–606.

Groisman, P. Y., and D. R. Legates, 1994: The accuracy of United States precipitation data, *Bull. Am. Meteorol. Soc.*, ***75***(2), 215–227.

Locatelli, J.D., and P.V.Hobbs, 1974: Fallspeeds and masses of solid precipitation particles, *J.Geophys.Res.*, 79, 2185-2197

Marshall, J. S., R. C. Langille, and W. M. Palmer, 1947: Measurements of Rainfall by
Radar, *J. Meteor.*, **4**, 186-192

Marshall, J.S. and W. M. Palmer, 1948: The distribution of raindrops with size. *J. Atmos. Sci.*, **5**, 165-166

Mote, P., A. Hamlet, M. Clark, and D. Lettenmaier, 2005: Declining Mountain Snowpack in Western North America. *Bull. Amer. Meteor. Soc.*, **86**, 39-49.

Piechota, T., J. Timilsena, G. Tootle, and H. Hidalgo, 2004: The western U.S. drought:
How bad is it? *Eos, Trans. Amer. Geophys. Union,* **85**, 301-308.

Rasmussen, R. M., J. Hallett, R. Purcell, J. Cole, and M. Tryhane, 2002: The Hotplate
Snowgauge. *11th Conf. on Cloud Physics*, Ogden, UT, Amer. Meteor. Soc., P1.6.

Rasmussen, J. Hallett, M. L. Tryhane, S.D. Landolt, R. Purcell, M.C. Beaubien,

Jeffries, W.Q., F. Hage, and J. Cole, 2005: The hotplate snow gauge, *13th Symposium on Meteorological Observations and Instrumentation*, Savannah, GA, June 20-24, 6.2.

Rasmussen, M. Dixon, S. Vasiloff, F. Hage, S. Knight, J. Vivekanandan, and

Xu, M., 2003: Snow Nowcasting Using a Real-Time Correlation of Radar Reflectivity with Snow Gauge Accumulation. *J. Appl. Meteor*, **42**, 20–36.

Sekhon, R.S and R.C.Shrivastava, 1970: Snow size spectra and radar reflectivity, *J. Atmos. Sci.*, 27, 299-307

Super, A. B., and E. W. Holroyd, 1998: Snow accumulation algorithm for the
WSR-88D radar: Final Report. Bureau of Reclamation Report R-98-05, Denver, CO, July, 75.

Wolfe, J.P., Radar-estimated Upslope Snowfall Rates in Southeastern Wyoming, MS thesis, Dept. of Atmospheric Science, University of Wyoming, May 2007

Young, H.D.,1962: *Statistical Treatment of Experimental Data*, McGraw-Hill, New York, New York.